Effect of pH on the properties of ZnO nanostructures prepared by chemical bath deposition method

L F Koao[1], F B Dejene[1] and H C Swart[2]

[1]Department of Physics, University of the Free State (Qwaqwa Campus), Private Bag X13, Phuthaditjhaba, 9866, South Africa
[2]Department of Physics, University of the Free State, P.O. Box 339, Bloemfontein, 9300, South Africa.

E-mail: koaolf@ufs.ac.za

Abstract. ZnO powders were prepared by chemical bath deposition method by varying the pH of the precursor. Different amount of ammonia hydroxide were added to change the pH of the solution from 5 to 12 values. The effect of pH of the precursor on the structure, morphology, optical and luminescence properties of ZnO nanostructures were investigated. The X-ray diffraction (XRD) patterns of the ZnO nanostructures correspond to the various planes of a single hexagonal ZnO phase. It was observed that the diffraction peaks increased in intensity with an increase in pH. The estimated average grain sizes calculated using the XRD spectra were found to be in the order of 38 ± 1 nm. It was observed that the estimated average grain sizes increased slightly with an increase in pH. The surface morphology study revealed that the grains were flakes-likes at low pH (< 6) but flower-like for high pH (12). The UV-Vis spectra showed a red shift with an increase in pH. The band gap energy of ZnO was found to decrease but the luminescence intensities increased with an increase in pH values. PL showed that the ultra-violet emission intensity of the nanostructures decreased with an increase in pH but the visible emission increased with an increase in pH.

1. Introduction

Nowadays, zinc oxide (ZnO) is a very attractive material in numerous promising applications such as gas sensors, photocatalyst, biosensnsres, solar cells, electrical and optical devices due to its non-toxic material with a wide direct band gap (3.37 eV) and a large exciton binding energy (60 meV) [1]. ZnO practical application is decided by its properties which can be modulated by varying its morphology [2-3]. A number of ZnO nanostructures such as nano wires [4], nanorods [5], nanotube [6], nanobelts [7], nanoflower-like [3], nanoplates [8], tetrapod [9] and nanoparticles [10] have been reported. Numerous methods have been employed for the production of ZnO nanostructures such as vapor liquid solid (VLS) [11], sol–gel method [12], Ball milling (BM) [10], and combustion method [13]. Some of these synthetic processes require long reaction time, high synthesis and annealing temperatures. To avoid some of these challenges the chemical bath deposition (CBD) method was used, is a simple, cheap and convenient process to prepare semiconducting materials. The more recent interest in all things 'nano' has provided a boost for CBD, since it is a low temperature, solution (almost always aqueous) technique and it gives better homogeneity. The aim of this paper was to investigate the effect of pH on the structure, morphology, optical and luminescence properties of the ZnO. Nesakumar et al. [14] prepared ZnO nanoparticles at different pH values under harsh conditions. Change in shape from nanosphere to nanorods was observed by varying pH from 11 to 10.7. Other researchers [15] showed that as pH increases the luminescence intensity in the UV region increases. From our work, we were able to observed the change of X-ray diffraction (XRD) structure from $Zn(OH)_2$ to hexagonal ZnO by increasing the pH.

2. Experimental

The pH of the bath was controlled by varying different volumes of ammonia. The ZnO powders were prepared by holding volumes of zinc acetate and thiourea constant and varying the volumes of ammonia in the precursor. Ammonia was used as a complexing agent. The 0.46 M of zinc acetate was dissolved in 500 mL of deionized water. 0.18 M thiourea was dissolved in 500 mL of deionized water and 123.5 mL of ammonia were dissolved in 500 mL of deionized water. Then a magnetic stirrer was used to stir each of the mixtures for overnight at room temperature to ensure homogenous distribution of the solution reagents. The amount of each solution was taken in the following order: 60 mL quantity of zinc acetate was first added to the beaker which was placed in the water bath, followed by addition of 60 mL of thiourea solution and the mixture was stirred for 30 s, following that, 5 mL of ammonia solution was then added slowly in the mixture, while continuously stirring for 5 min. The pH measured was 5. Water bath was maintained to be at a constant desired temperature of 80 ºC. The precipitates were then left overnight and filtered thereafter. The precipitates were later washed with 60 mL of ethanol and secondly with 60 mL of acetone. The obtained precipitates were dried at ambient conditions for 3 days. After that the powders were ready to be characterized. The synthesis of ZnO nanostructures in the presence of different volumes of was performed similarly. The varied amounts of ammonia present in the precursor solution are 24 mL, 60 mL, and 75 mL, the pH measured for each mixture were 6, 8 and 12, respectively. The particle size and morphology and the structural and luminescent properties of the as-synthesized phosphors were examined by means of Scanning Auger electron microscopy (SAM) using a PHI 700 Scanning Auger Nanoprobe, X-ray diffraction (XRD), Uv-vis spectroscopy and Photoluminescence (PL).

3. Results and Discussion

3.1 Structural analysis and Composition analysis

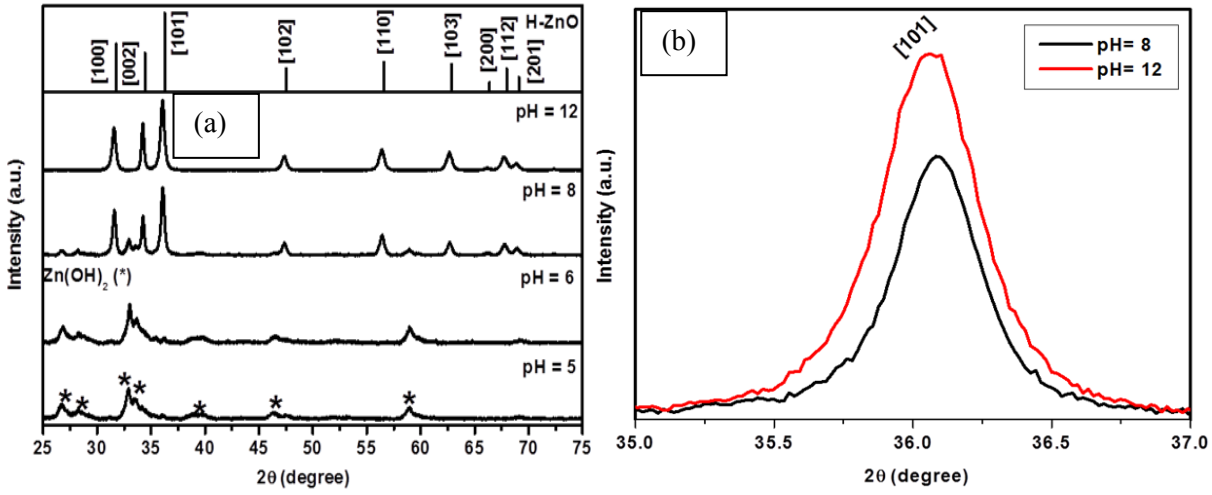

Figure 1. X-ray powder diffraction patterns for $Zn(OH)_2$ and ZnO structures prepared at (a) various pH and (b) XRD patterns at (103).

Figure 1 (a) shows the XRD patterns of the $Zn(OH)_2$ and ZnO nanostructures synthesised at various pH. One can see that at low pH the XRD structure was for $Zn(OH)_2$ [16], when the pH was increased further the structure changed to hexagonal ZnO. By increasing the pH using ammonia the $Zn(OH)_2$ peaks diminished. It is suggested that those peaks that are marked with star (*) are related to the $Zn(OH)_2$ as confirmed by the JCPDS no: 38-0356 [17]. The hexagonal ZnO match perfectly with the data of Koao et al. [3]. The average crystallite size of the as-prepared crystals can be estimated from the Full Width Half Maximum (FWHM) of the diffraction peaks using the Debye formula [18]. The

average crystallite sizes estimated using the XRD spectra were found to be 50 and 43 nm for samples synthesized at pH of 12 and 8, respectively. The estimated average grain size increased with an increase in the pH. The increase in estimated crystallite size may be due the zinc hydroxide that dissolves as the PH increases which are the primary precursor for growth of ZnO that lead to the formation of bigger crystallite. The average estimated values of the cell constants of *a* and *c* are 3.26979 and 5.23373 Å and 3.26727 and 5.23092 Å for pH= 8 and pH= 12, respectively. The estimated lattice parameters match perfectly with standard data available in JCPDS card no. (36-1451, a = 3.24982 and c= 5.20661 Å). It is clear that the estimated lattice parameters decreased with an increase in pH. This may be due to the increase in estimated crystallite sizes. In Figure 1(b), it was observed that the XRD diffraction intensities increased with an increase in pH, implying that the crystallite sizes increased and the improvement of the crystallinity.

3.2 Surface morphological analysis

Figure 2 (a), (b) and (c) show SEM images of the as prepared $Zn(OH)_2$ and ZnO nanostructures, respectively prepared at various pH but synthesized at constant time and bath temperature. At low pH of 5 the surface aspects of the SEM image was composed of flakes-like structures. It is clear that at the pH of 8, the morphology consists of mixtures of flakes-like and flower-like structures. However, by further increasing the pH to 12, morphology consists of flower-like structures surrounded by few spherical nanoparticles. By comparing the SEM micrographs it is clearly seen that by increasing the pH using ammonia the flake-like changed to the flower-like structures. The change in morphology may be due to the increasing pH inducing the nucleation growth yielded the flower-like structures.

AES measurements were carried out to check the elements and to evaluate their purity. The Auger spectrum of the $Zn(OH)_2$ and ZnO are shown in Figure 3. The typical spectrum of the nanoflowers confirmed the presence of Zn and O. The signals at energy of 276 eV are ascribed to the presence of adventitious carbon, which come from the atmosphere and due to handling. The Zn and O concentration were relatively very low for the sample synthesized at pH of 5 compared to the sample prepared at pH of 8 and 12. Moreover, no other impurities were found on the surface of the ZnO, suggesting that the as-synthesized ZnO were relatively pure.

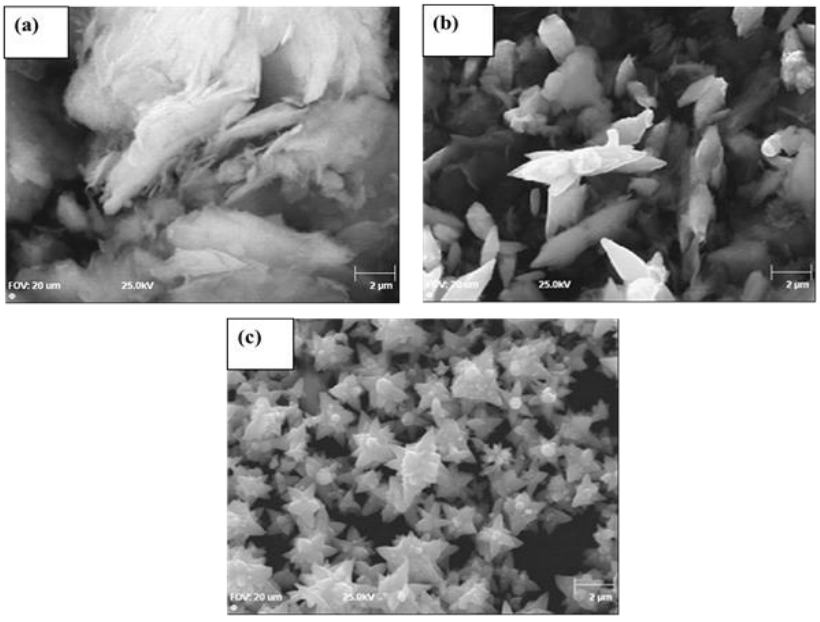

Figure 2. SEM images of $Zn(OH)_2$ and ZnO nanostructures for pH of (a) 5, (b) 8 and (c) 12 synthesized by CBD at bath temperature of 80 ºC.

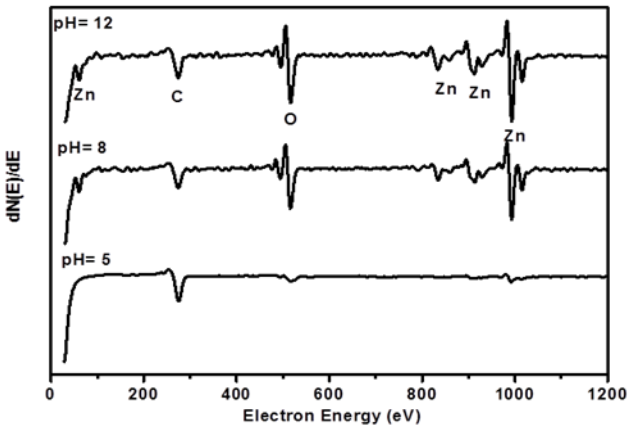

Figure 3. Auger spectra of the $Zn(OH)_2$ and ZnO powders prepared at pH= 5, pH= 8 and pH= 12 using the CBD method.

3.3 Optical properties

The UV-visible reflectance spectra of the as prepared samples are illustrated in Figure 4(a). It clearly indicates that by increasing pH, the optical absorption edge shifted to a higher wavelength. At low pH the absorption edge is at around 261 nm, which may be due to the presence of $Zn(OH)_2$ as confirmed by XRD analysis. The absorption edges are homogeneous, no other band was observed in the high pH of 12, which confirmed that the synthesized sample was pure ZnO.

The energy band gap of these materials was estimated using the Kubelka-Munk remission function **[19].** In Figure 4(b) it can be seen clearly that the band gap energy of the ZnO nanostructures decreased slightly with an increase in the pH. The estimated band gap energy for the synthesis time were 3.36 ± 0.01, 3.31 ± 0.01 eV for flower-like ZnO synthesized for pH of 8 and 12, respectively. All the calculated band gap energies were below the theoretical band gap value of 3.37 eV at room temperature. This may be due to an increase in grain size as confirmed by XRD analyses [20].

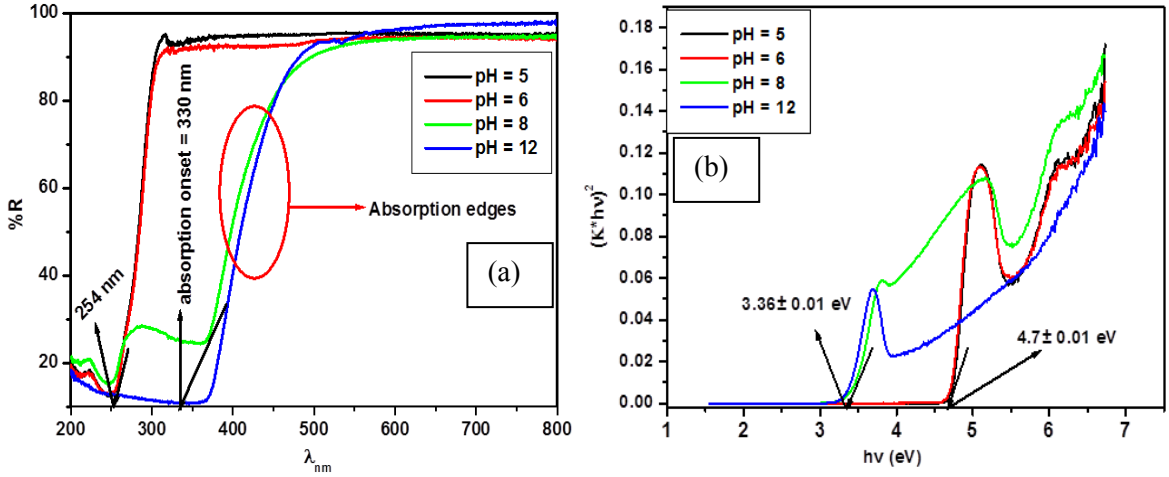

Figure 4. The absorbance spectra (a) and the band gap energy (b) of the $Zn(OH)_2$ and ZnO structures prepared at different pH.

It is known that as the grain size increased, the electronic states are not discrete and results in the reducing of the band gap and decreased the oscillator strength [21]. The highest band gap energy was

obtained for the sample synthesized at low pH, with its estimated band gap energy of 4.70 ± 0.01 eV. The band gap energy may be due to the $Zn(OH)_2$.

3.4 Photoluminescence

Figure 5 shows the photoluminescence (PL) spectra of the $Zn(OH)_2$ and ZnO nanostructures synthesized at different pH with the excitation wavelength at 300 nm. The excitation wavelength was taken from absorption onset on reflectance results. Four obvious luminescence peaks in the UV region were observed at around 364, 379, 414 and 450 nm from both low pH of 5 and 6. Those luminescence peaks at around 364 and 379 nm are usually ascribed to the radiative recombination of ZnO free excitons [22]. They are both attributed to the transition from valence band to conduction band of ZnO semiconductors. A violet peak at around 414 nm was ascribed as the emission from zinc vacancies present in the ZnO lattice [23]. The blue emission centred at 450 nm may be due to the electron transition from Zn_i to V_{zn} [22]. By increasing the pH further, those peaks decreased in luminescence intensity and a known yellow emission peak started to emerge at around 570 nm. This yellow emission was due to the presence of oxygen interstitial in the synthesized material [17]. The emission peak in the visible region increased in luminescence intensity with an increase in pH. The decreased in luminescence intensity in UV region may be due to an increase in estimated crystallite size as confirmed by the XRD [20]. The increase in the visible emission as the pH increased may be due to the reduction of $Zn(OH)_2$ as confirmed by the XRD analysis. The low pH provided enough ionization energy and increased the concentration of $Zn(OH)_2$, strengthening the UV to blue emissions. The high pH induced the outward diffusion of $Zn(OH)_2$ and quenching the UV to blue emissions. It was very interesting to observe that the XRD, SEM, XPS, UV and PL results support each other.

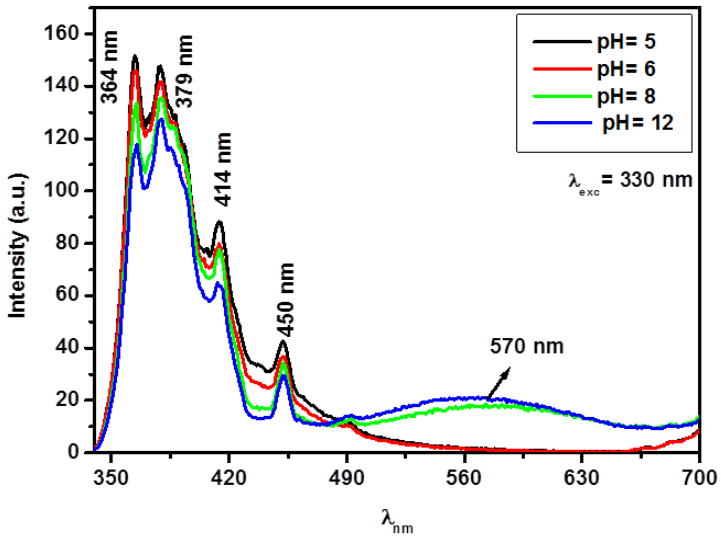

Figure 5. The PL spectra of ZnO nanostructures, prepared at different pH of pH= 5, pH= 8 and pH= 12 using the CBD method.

4. Conclusion

The ZnO nanostructures have been successfully synthesized by the chemical bath deposition technique at 80°C by varying the pH using ammonia. XRD showed that the structure of the material changed from $Zn(OH)_2$ to the hexagonal wurtzite ZnO. XPS showed that the amount of oxygen and Zn increased with an increase in pH. UV spectroscopy showed that the band gap energy of the ZnO flower-like decreased with an increase in the pH. PL showed that the visible emission intensity of the nanostructures increased with an increase in pH.

Acknowledgement
The author would like to acknowledge the National Research Foundation and the University of the Free State for financial support.

Reference

[1] Heo S N, Park K Y, Seo Y J, Ahmed F, Anwar M S, Koo B H 2013 *Electro. Mater. Lett.* **9** 261-265.
[2] Park W I, 2008 *Met. Mater. Int.* **18** 659.
[3] Koao L F, Dejene B F, Swart H C, Botha J R 2013 *J. Lumin* **143** 463-468.
[4] Amiruddin R, Kumarn M C S, 2014 *Ceram. Int.* **40** 11283–11290.
[5] Srivatsa K M K, Chhikara D, Kumar M S, 2011 *J. Mater. Sci. Technol*. **27** 701–706.
[6] Angwafor N G N, Riler D J, 2008 *Phys. Status Solid A.* **205** 2351-2354.
[7] Gao P X, Ding Y, Mai W J, Hughes W L, Lao C S, Wang Z L, 2005. *Sci*. **309** 1700-1704.
[8] Molefe F V, Koao L F, Dolo J J, Dejene B F, 2014, *Physica B*. **439** 185-188.
[9] Feng L, Liu A, Liu M, Ma Y, Wei J, Man B, 2010, *Mater. Character*. **61** 128-133.
[10] Amirkhanlou S, Ketabchi M, Parvin N, 2012, *Mater. Lett*. **86** 122-124.
[11] Huang M H, Wu Y Y, Feick H, Tran N, Weber E, Yang P H, 2001, *Adv. Mater*. **12** 113-116.
[12] Zhang C, 2010, *J. Phys. Chem. Solids*. **71** 364-369.
[13] Lamas D G, Lascalea G E, Walsoc N E 1998 *J. Eur. Ceram. Soc*. **18** 1217–1221.
[14] Nesakumar N, Rayappan J B B, Jeyaprakash B G, Krishnan U M, 2012, *J. Appl. Sci*. **12** 1758-1761.
[15] Yuan H, Xu M, Huang Q Z, 2014, *J. Alloy. Comp*. **616** 401-407.
[16] Jia W, Dang S, Liu H, Zhang Z, Yu C, Liu X, Xu B, 2012, *Mater. Lett*, **82** 99-101.
[17] Peng W Q, Qu S C, Cong G W, Wang Z G, 2006, *Mater. Sci. Semi. Process*, **9** 156-159.
[18] Cullity B D1978, 1956*Elements of X-ray Diffraction (2nd Ed)*, (Addison Wesley) 285-284.
[19] Molefe F V, Koao L F, Dejene B F, Swart H C,2015, *Optical. Mater*. **46** 292–298.
[20] Farhadi-Khouzani M, Fereshteh Z, Loghman-Estarki M R, Razavi R. S, 2012, *J. Sol-Gel Sci. Technol*, **64** 193-199.
[21] Sahu S N, Nanda K K, 2001, Proc. *Indian Natl. Sci. Acad*. **67 (A)** 103-130.
[22] Wang Y F, Yao J H, Jia G, Lei H, 2011, *Acya Physica Polonica A*, **119 (3)** 451-454.
[23] Lin B, Fu Z, Jia Y, 2001, *Appl. Phys. Lett*. **79** 943-945.